ORGANIZATION FOR NUCLEAR RESEARCH

PRODUCTION OF ψ AND ψ' MESONS IN π^-N SCATTERING AT 150 GeV/c

M.A. Abolins*), R. Barate**), P. Bareyre, P. Bonamy, P. Borgeaud, J.C. Brisson, M. David, J. Ernwein, F.X. Gentit, G. Laurens, Y. Lemoigne, J. Pascual, J. Poinsignon, A. Roussarie, G. Villet and S. Zaninotti

CEN-Saclay, Gif-sur-Yvette, France

P. Astbury, A. Duane, G.J. King, D.P. Owen, D. Pittuck, D.M. Websdale, M.C.S. Williams and A. Wylie**)

Imperial College, London

J.G. McEwen

Southhampton University

B. Brabson, R. Crittenden, R. Heinz, J. Krider, T. Marshall, R.McIlwain***), and T. Palfrey***)

Indiana University, Bloomington, Indiana, USA

In a large-acceptance spectrometer, muon pairs and associated hadrons were observed with $\mu\mu$ masses up to 10 GeV/c^2 and $\Delta M/M = 0.015$ resolution. We report here on the production of 4000 ψ and 80 ψ' mesons.

Geneva - 3 November 1978

(Submitted to Physics Letters B)

---

*) On leave from Michigan State University, East Lansing, Michigan, USA.

**) Present address: CERN, Geneva, Switzerland.

***) On leave from Purdue University, West Lafayette, Indiana, USA.

At the CERN Super Proton Synchrotron (SPS) we have performed an experiment with a large-acceptance spectrometer to look at the hadrons associated with lepton pairs ($\mu^+\mu^-$ or e^+e^-) produced in π^-Be scattering at 150 GeV/c*). We report here on the production of 4000 ψ and 80 ψ' mesons which we have observed in our $\mu^+\mu^-$ data. We find that ψ and ψ' production is of hadronic origin. We observe Feynman x distributions (x_F) which suggest that the valence quarks are crucial components of the production process for the ψ and ψ'. We find a transverse momentum (p_T) distribution for the ψ which flattens as p_T approaches zero. We show that the ψ production may be due to charmed quark fusion.

The experimental set-up is shown in fig. 1. The 150 GeV/c π^- beam was produced at 0° by the 210 GeV/c external proton beam of the CERN SPS. The beam intensity was 6×10^6 π^-/burst. A copious muon halo (1.5×10^6 μ/m^2/burst) accompanied the beam and was detected by two sets of veto counters. Two scintillator hodoscopes were used to steer the beam onto the Be targets and to suppress beam pile-up. The three Be targets had a total length of 16.4 g/cm^2. The spectrometer subtended angles of ±160 mrad vertically and ±250 mrad horizontally at the target. It was composed of 11 multiwire proportional chambers (MWPC) immersed in the magnetic field of the Goliath magnet. These MWPCs had a total of 42 sense planes, the vertical wires in the first two planes having a 1 mm pitch, and all other planes a 2 mm pitch. Goliath had a magnetic field of 1.5 T, a magnetic volume of 3.3 m^3, and a bending strength of 3.7 Tm. Following Goliath were three large MWPCs, each containing four planes of 3 mm pitch sense wires. (There was a total of 40,000 wires in the MWPCs.) After the first large MWPC was a 28-celled Čerenkov counter filled with CO_2 at atmospheric pressure. The third large MWPC was an integral part of an electron-gamma-ray calorimeter of the scintillator-lead sandwich type. Finally, there was a muon filter composed of 2380 g/cm^2 of

---

*) About 40% of our data were taken at 140 GeV/c beam momentum. We have combined these with our 150 GeV/c data as no significant difference was observed when the two data sets were analysed separately.

iron sandwiched between two sets of hodoscopes. These hodoscopes had central horizontal gaps corresponding to vertical angles of ±20 mrad at the target.

Our experiment was designed to measure and identify the particles produced in association with the ψ. This required that the muon iron shield be placed well downstream of the production target, in contrast to beam dump experiments [1-4]. To suppress the μ background from π and K decays at the trigger level, we exploited the fact that the ψ mass is large compared to the "background mass". Low-momentum muons (< 5 GeV/c) were swept away by the magnet or stopped in the iron. Since the muons of interest had opposite charges, the trigger was made on diagonally opposite quadrants of the hodoscopes; this, combined with the gaps in the hodoscopes, imposed a minimum laboratory angle requirement of 40 mrad between the muons. This resulted in a trigger which was not very sensitive to dimuon masses below 1 GeV. An additional trigger requirement came from using the hodoscopes to ensure that the muons pointed towards the target in the vertical plane. The trigger rate was 6×10^{-6}/incident pion.

Figure 2a shows the dimuon mass spectrum corrected for geometrical acceptance but not for the contribution from π and K decays. The smooth curve is a fit to our data from 2.2 to 10.0 GeV using a sum of two exponentials and two Gaussians. The fitted ψ and ψ' masses are 3.097 ± 0.001 and 3.680 ± 0.004 GeV, respectively. The standard deviations of 46 ± 1 and 54 ± 7 MeV are consistent with our mass resolution. Approximately 60% of the small background under the ψ comes from prompt muon pairs, as determined by an analysis of like-sign muons*). The rest of the background comes mainly from π and K decays. Assuming a linear dependence of the cross-section with A, we determine a cross-section per nucleon for the ψ and ψ' of 95 ± 10 and 15 ± 4 nb. The errors include effects due to statistics, acceptance uncertainties, and detector inefficiency. The ratio of the ψ' and ψ cross-sections, (16 ± 3)%, is approximately the same as that observed at $\sqrt{s}$ = 64 GeV [5].

---

*) We will present our prompt muon continuum results in a future publication.

These results can be used to determine whether the production of ψ and ψ' are of an electromagnetic origin [5]. If the production in $\pi^- p$ interactions were electromagnetic, one could expect the ratio

$$R_{\pi^- p}^{\psi,\psi'} = \frac{B\sigma_{\pi^- p}^{\psi,\psi'}}{(d\sigma^c/dM)_{M=M_\psi, M_{\psi'}}}$$

to be equal to the ratio

$$R_{ee}^{\psi,\psi'} = \frac{\int B\sigma_{ee}^{\psi,\psi'}\, dE}{\sigma(e^+e^- \to \mu^+\mu^-)} .$$

Here $\sigma_{\pi^- p}^{\psi,\psi'}$ is the inclusive cross-section for ψ and ψ' in πp collisions, and $(d\sigma^c/dM)_{M=M_\psi, M_{\psi'}}$ is the cross-section of the prompt $\mu\mu$ continuum interpolated under the ψ and ψ'; B is the ψ or ψ' $\mu^+\mu^-$ branching ratio [6]. R_{ee} has been measured [7] at e^+e^- colliding rings to be $R_{ee}^{\psi} = 0.092$ GeV and $R_{ee}^{\psi'} = 0.006$ GeV. In our experiment we find $R_{\pi^- p}^{\psi} = 6.65/0.66 = 10.1 \pm 3$ GeV and $R_{\pi^- p}^{\psi'} = 0.12/0.346 = 0.35 \pm 0.14$ GeV. This result indicates that most of the ψ and ψ' production is of hadronic origin.

Figures 2b and 2c show the distributions in x_F and p_T for the ψ and ψ'. The effect of the background under the ψ, ψ' peaks has been corrected using the events in the neighboring mass zones. The x_F and p_T resolutions are approximately 0.004 and 25 MeV/c. The x_F distributions are well fitted by

$$\frac{d\sigma}{dx_F} = b\ (1 - |x_0 - x_F|)^c .$$

The results of our calculations are given in table 1. Both distributions are significantly shifted from $x_F = 0$.

We fit the p_T distributions $(1/p_T)(d\sigma/dp_T)$ with an exponential in p_T, an exponential in p_T^2, and $[1 + (p_T/B)^2]^C$. For the ψ, the non-exponential fit is the best; it can accommodate the flattening of the cross-section at small p_T while fitting the high p_T data. We find $B = 1.9 \pm 0.2$ GeV/c and $C = -4.5 \pm 0.5$. All fits give the same $\langle p_T \rangle$ for the ψ: 1.00 ± 0.02 GeV/c; for the ψ', $\langle p_T \rangle = 0.89 \pm 0.17$ GeV/c.

In fig. 3 we show the angular distribution of the ψ decay muons (corrected for background effects) in the Gottfried-Jackson frame. The data are from the region $0 \leq x_F < 0.4$ and $0.0 \leq p_T \leq 2.4$ GeV/c. This region was chosen to enable us to weight each event*). The smooth curve is a fit to $1 + \alpha \cos^2 \theta_{GJ}$. We find $\alpha = -0.13 \pm 0.18$. In the simple quark fusion model α can be written as

$$\alpha = \frac{1 - (4m^2/Q^2)}{1 + (4m^2/Q^2)} ,$$

where m is the quark mass and Q is the dimuon mass [8]. (If the quarks have transverse momentum, α would be damped by approximately 20% [9].) Quark fusion from light quarks would give $\alpha \approx 1$, while charmed quark fusion would have $\alpha \approx 0$. Thus our result is consistent with charmed quark fusion, but not with light quark fusion. (We assume that the $\psi q\bar{q}$ vertex has no structure [8].) Even if the ψ comes from decays $\chi \to \gamma\psi$, if the χ is produced by charmed quark fusion then the ψ still has $\alpha \approx 0$.

If ψ mesons are produced primarily by charmed quark fusion, the shift from zero of the x_F distribution implies that the momentum distribution of sea quarks is linked to that of the valence quarks [10,11]. Charmed quark fusion for the ψ leads to a prediction that charmed particles are produced in association with the ψ. We will attempt to see if this is true when we analyze all tracks in our spectrometer.

Table 1

Parameters of the x_F fits to the ψ and ψ' cross-sections

$\mu\mu$ mass region	b (nb)	c	x_0	χ^2/N
ψ	165 ± 18	2.5 ± 0.13	0.18 ± 0.01	1.7
ψ'	40 ± 11	3.9 ± 1.5	0.18 ± 0.03	0.2

*) Alternatively, one can assume a functional form for the cross-section and get an over-all geometrical efficiency for cos θ_{GJ} for all data. This technique was used for the x_F and p_T distributions, but was found to be model dependent for the cos θ_{GJ} distribution.

REFERENCES

[1] K.J. Anderson et al., Phys. Rev. Letters 37, 799 (1976).

[2] J.G. Branson et al., Phys. Rev. Letters 38, 1331 (1977).

[3] Yu.B. Bushnin et al., Phys. Letters 72B, 269 (1977).

[4] Yu.M. Antipov et al., Phys. Letters 72B, 278 (1977).

[5] A.G. Clark et al., Electron pair production at the CERN ISR, Submitted to Nuclear Physics B.

[6] Particle Data Group, Review of Particles Properties, Phys. Letters 75B, (1978), 1.

[7] G.S. Abrams, Proc. Intern. Symp. on Lepton and Photon Interactions at High Energies, Stanford, 1975 (SLAC, Stanford, Calif. 1975), p. 25.

[8] K.V. Vasavada, Phys. Rev. D16, 146 (1977).

[9] E.L. Berger, J.T. Donohue and S. Wolfram, Phys. Rev. D 17, 858 (1978).

[10] A. Donnachie and P.V. Landshoff, Nuclear Phys. B112, 233 (1978).

[11] Y. Kinoshita and K. Kinoshita, Production mechanism of the J particle in hadrons collisions, BI-TP 77/11 (1977).

Figure captions

Fig. 1 : Experimental layout. H represents a scintillator hodoscope; μ is a muon beam halo detector.

Fig. 2 : a) Dimuon mass spectrum corrected for geometrical acceptance.

b) and c): x_F distribution for the ψ and ψ', respectively.

d) and e): p_T distribution for the ψ and ψ', respectively. The curves are described in the text. For d) and e) the dashed line is the exponential in p_T, the dotted line is the exponential in p_T^2, and the solid line is the non-exponential fit to the data.

Fig. 3 : Distribution of the cosine of the Gottfried-Jackson angle for 2880 ψ events. The smooth curve is a fit to the data of the form $1 + \alpha \cos^2 \theta_{GJ}$, with $\alpha = -0.13 \pm 0.18$.

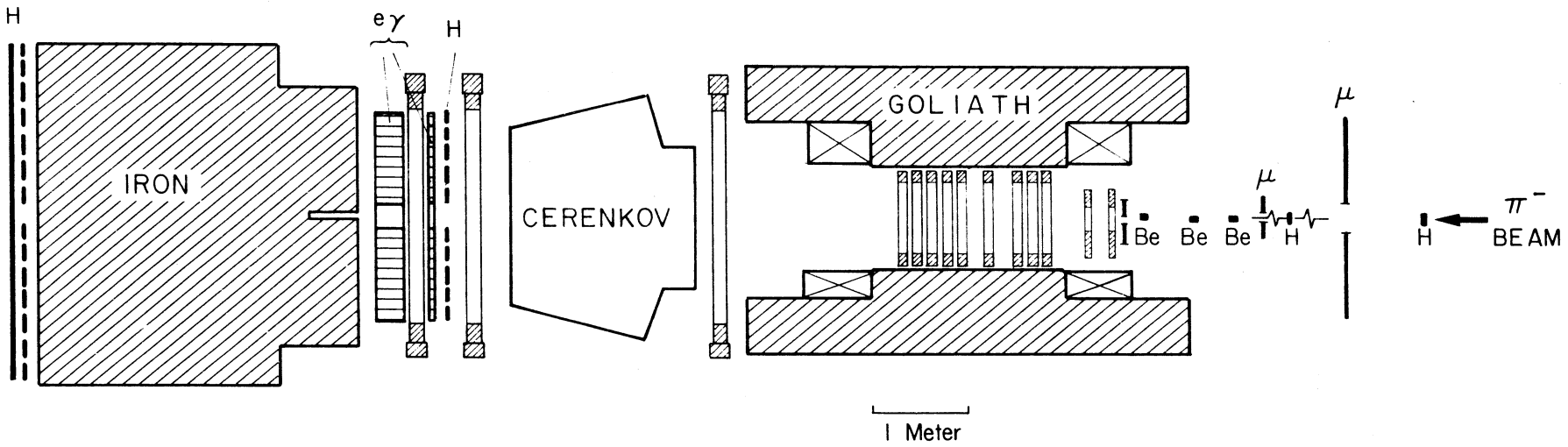

Fig. 1

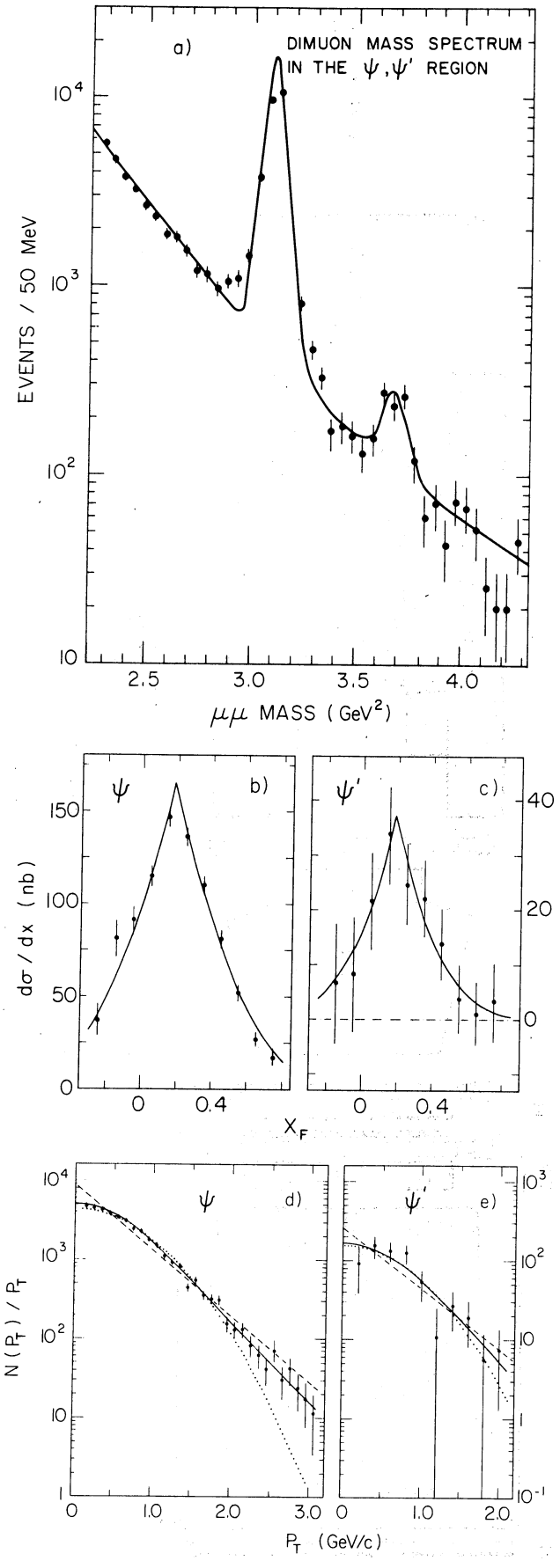
a)
DIMUON MASS SPECTRUM
IN THE ψ,ψ' REGION
EVENTS / 50 MeV
μμ MASS (GeV²)
ψ
b)
ψ'
c)
dσ / dx (nb)
X_F
ψ
d)
ψ'
e)
N(P_T) / P_T
P_T (GeV/c)

Fig. 2

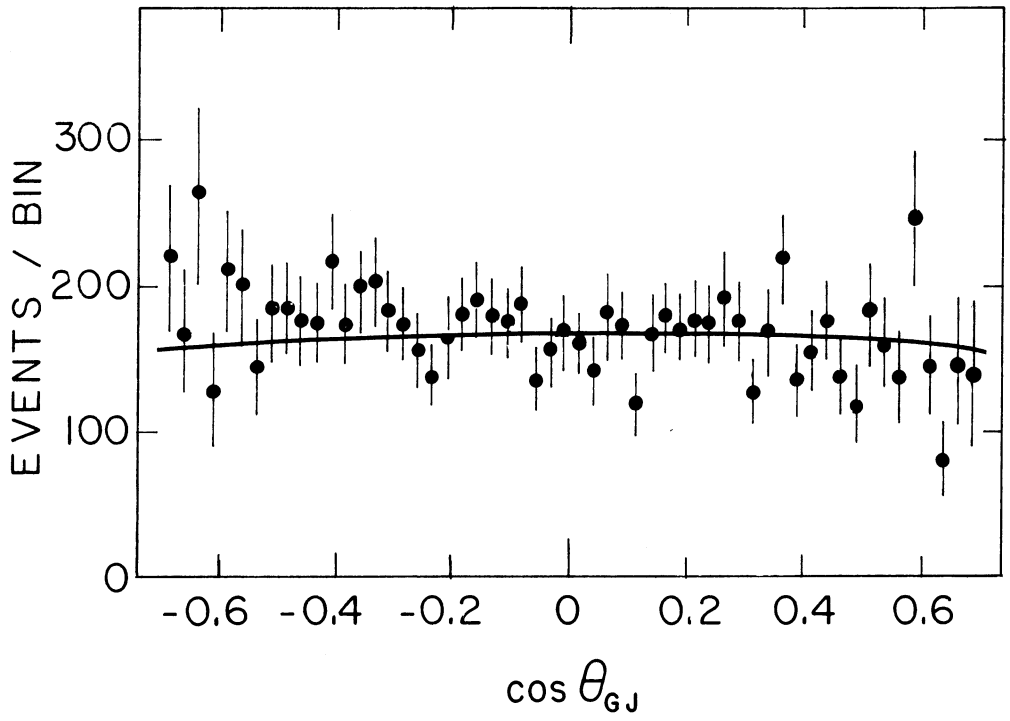

Fig. 3